Conformation of Solvent *N*,*N*-Dimethylpropionamide in the Coordination Sphere of the Zinc(II) Ion Studied by Raman Spectroscopy and DFT Calculations

Yasuhiro Umebayashi,[†] Babara Mroz,[‡] Mitsunori Asada,[†] Kenta Fujii,[†] Kai Matsumoto,[†] Yutaka Mune,[†] Michael Probst,[‡] and Shin-ichi Ishiguro*,[†]

Department of Chemistry, Faculty of Science, Kyushu University, Hakozaki, Higashi-ku, Fukuoka, 812-8581, Japan, and Institut für Ionenphysik, Universität Insbruck, Technikerstrasse 25, 6020, Insbruck, Austria

Received: November 16, 2004; In Final Form: April 11, 2005

Solvation structure of the zinc(II) ion in *N*,*N*-dimethylpropionamide (DMPA) was studied by Raman spectroscopy at varying temperature and by quantum mechanical calculations. No significant ion-pair formation was found for the $Zn(ClO_4)_2$ solution in the molality range $m_{Zn} < 1.5$ mol kg^{-1}, and the solvation number of the zinc(II) ion was determined to be 4, indicating that 6-coordination of DMPA is sterically hindered. Interestingly, DMPA molecules are under equilibrium between planar cis and nonplanar staggered conformers, and the latter is more preferred in the coordination sphere, while the reverse is the case in the bulk. The $\Delta G°$, $\Delta H°$, and $T\Delta S°$ values of conformational change from planar cis to nonplanar staggered in the coordination sphere were obtained to be −0.9, −8.5, and −7.5 kJ mol^{-1}, respectively. Density functional theory (DFT) calculations show that the planar cis conformer is more favorable than the nonplanar staggered one in the 1:2 cluster, as is the case for a single DMPA molecule and $H(DMPA)^+$, indicating that there hardly occurs solvent−solvent interaction through the metal ion in the Zn^{2+}−DMPA 1:2 cluster. On the other hand, the SCF energy of $[Zn(\text{planar } \textit{cis}\text{-DMPA})_{4-n}(\text{nonplanar staggered DMPA})_n]^{2+}$ ($n = 0-4$) decreases with increasing n, implying that the nonplanar staggered conformer is preferred in the solvate ion. It is thus concluded that solvent−solvent interaction through space, or solvation steric effect, plays a crucial role in the conformational equilibrium in the coordination sphere of the four-solvate metal ion.

Introduction

Much effort has so far been devoted to elucidate properties[1] and structures[2−6] of ion solvation. It has been established that metal-ion complexation depends strongly on the nature of solvent, such as dielectric constant, electron-pair donating and accepting abilities, and hydrogen-bonding property. The metal-ion complexation in nonaqueous solvents further depends on the molecular geometry of the solvent.[7,8] The bulkiness of solvent, particularly in the vicinity of the coordinating atom, plays an essential role in the solvation structure of the metal ion.[7−10] Indeed, it has been found that the metal−ion complexation with simple halide and *pseudo*halide ions is generally enhanced in *N*,*N*-dimethylacetamide (DMA) over *N*,*N*-dimethylformamide (DMF), despite physicochemical properties of the solvents being similar.[11−22] Also, the complexation is significantly enhanced in hexamethylphosphoric triamide (HMPA) over DMF, and the solvation number of a metal ion decreases in HMPA relative to DMF, indicating a *strong solvation steric effect* operates in HMPA.[23−27] Solvation steric effect also modifies an aspect of preferential solvation (*sterically controlled preferential solvation*) of a metal ion in solvent mixtures.[28−32]

According to our Raman spectroscopic study,[31,32] *N*,*N*-dimethylpropionamide (DMPA) exists as either planar cis or nonplanar staggered conformer in the bulk, as shown in Chart 1, and the former is enthalpically more favorable by ca. 5 kJ mol^{-1} than the latter. On the other hand, in the coordination sphere of the manganese(II) ion, the planar cis conformer is less favorable by ca. 11 kJ mol^{-1} than the nonplanar staggered one. The solvation number of the manganese(II) ion in *N*,*N*-dimethylpropionamide (DMPA) is five,[31] indicating that six-coordination is sterically hindered. Note that, according to our density functional theory (DFT) calculation, the conformational change hardly occurs for the protonated DMPA, in which no solvation steric effect is expected. This implies that the solvation steric effect is still significant, even if the solvation number of the metal ion is decreased to five. To shed more light on the solvation steric effect of DMPA bound to the metal ion, we further examined the solvation structure of the zinc(II) ion in DMPA by Raman spectroscopy and DFT calculation. The zinc(II) ion is smaller than the manganese(II) ion, and the solvation number decreases even to four, as will be discussed later.

CHART 1

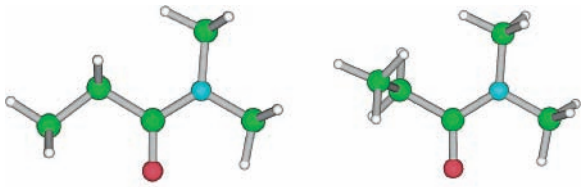

Experimental Section

Materials. All chemicals used were of reagent grade. The $Zn(ClO_4)_2$ hexahydrates were prepared from zinc carbonate and perchloric acid. A $Zn(ClO_4)_2$ DMPA solution was prepared by dissolving $Zn(ClO_4)_2$ hexahydrate crystals in DMPA. As the $Zn(ClO_4)_2$ DMPA solvate cannot be isolated, a small amount

[†] Kyushu University.
[‡] Universität Insbruck.

10.1021/jp044763a CCC: $30.25
Published on Web 05/06/2005

of water in the solution was removed by repeated evaporation of DMPA under a reduced pressure. Water content in the $Zn(ClO_4)_2$ DMPA solution thus prepared was found to be negligible by a Karl Fischer titration. Molality of the metal ion was determined by an EDTA titration. Neat DMPA was stored with molecular sieves 4Å for several weeks, and distilled under a reduced pressure. Water content was checked to be less than 100 ppm. All sample solutions were prepared in a glovebox under an atmosphere of argon, in which water content was kept within 1 ppm.

Measurements. Raman spectral measurements were carried out over the range 650−1000 cm^{-1}, using a dispersion Raman spectrometer (JASCO NR-1000) and an argon ion laser (COHERENT Inova 70) operating at 514.5 nm. The optical resolution was either 2.5 or 5.0 cm^{-1}. As no significant difference was found in the evaluation of the solvation number, data obtained with the optical resolution of 5.0 cm^{-1} were used for the analyses throughout. A $Zn(ClO_4)_2$DMPA solution was titrated with neat DMPA by using an autoburet (KEK APB-410), and spectral data were recorded on a personal computer at each titration point. Raman spectral measurements at varying temperature were carried out with an FT-Raman spectrometer (Perkin-Elmer GX-R) equipped with an Nd:YAG laser operating at 1064 nm. The employed optical resolution was 4 cm^{-1}. A sample solution in a quartz cell was thermostated within ±0.3 K at a given temperature during the measurement. The sample room was filled with dry nitrogen gas to avoid condensation of moisture on the surface of the cell at low temperature.

Data Analysis. Raman spectra obtained over a given frequency region were deconvoluted to extract single Raman bands. A single Raman band is assumed to be represented as a *pseudo*-Voigt function, $f_V(\nu) = \gamma f_L(\nu) + (1 - \gamma) f_G(\nu)$, where $f_L(\nu)$ and $f_G(\nu)$ stand for Lorentzian and Gaussian components, respectively, and the parameter γ ($0 < \gamma < 1$) is the fraction of Lorentzian component. To avoid uncertainty in obtaining the γ value of the bound peak at lower metal-ion molality, the value was fixed to that at the highest metal-ion molality. The intensity I of a single Raman band is evaluated according to $I = \gamma I_L + (1 - \gamma) I_G$, where I_L and I_G denote integrated intensities of the Lorentzian and Gaussian components, respectively. A curve-fitting nonlinear least-squares program RAMCAL, which is based on the Marquardt−Levenberg algorithm,[33,34] was developed in our laboratory and used throughout analyses.

In the $Zn(ClO_4)_2$ solutions examined, the ν_1 band of the perchlorate ion at 933 cm^{-1} was used as an internal standard, as the perchlorate ion hardly forms ion-pairs under the experimental conditions examined here. Indeed, no appreciable change in the ν_1 band parameters was found by varying the temperature. The ν_1 band intensity plotted against the salt molality fell on a straight line to give Raman scattering coefficient J as the slope. The J value in water has been reported in the litereature.[35] Raman scattering coefficients for solvent were then evaluated on the basis of the J value of the ν_1 band obtained for 1 mol kg^{-1} ClO_4^- ion in DMPA. A Raman band of free solvent in the bulk shifts when the solvent binds to the metal ion. If solvent involves a single conformer, the intensity of free solvent I_f decreases and that of bound solvent I_b increases with increasing molality m_{Zn}. If no ion-pair forms, the following relationship holds between I_f and m_{Zn}:

$$I_f = m_T J_f - n J_f m_{Zn} \quad (1)$$

where m_T, J_f, and n stand for the total molality of solvent, the scattering coefficient of the free solvent, and the solvation number, respectively. Plots of measured I_f against m_{Zn} give a straight line with the intercept α ($=m_T J_f$) at $m_{Zn} = 0$ and the slope β ($=nJ_f$). As m_T is known, J_f and n are given by α/m_T and β/J_f, respectively. Similarly, the Raman scattering coefficient of the bound solvent J_b is obtained from the slope of the I_b vs m_{Zn} plot, according to the relationship $I_b = nJ_b m_{Zn}$.

As DMPA involves in fact two conformers, total molality of solvent m_T is represented as $m_T = m_{nps} + m_{pc} + (n_{nps} + n_{pc})m_{Zn}$, where m_{nps} and m_{pc} denote molality of free nonplanar staggered (nps) and planar cis (pc) conformers in the bulk solvent, respectively, and n_{nps} and n_{pc} stand for the average number of respective conformers bound to the metal ion. Here, we define equilibrium constant $K_f = m_{nps}/m_{ps}$, and intrinsic scattering coefficients according to $I_{f,nps} = J_{f,nps} m_{nps}$ and $I_{f,pc} = J_{f,pc} m_{pc}$ for respective conformers in the bulk, where $I_{f,nps}$ and $I_{f,pc}$ are band intensities. Measured intensity $I_{f,pc}$ of the 760 cm^{-1} band is plotted against m_{Zn} to obtain the intercept $\alpha_{f,pc}$. The $J_{f,pc}$ value is thus given by $J_{f,pc} = \alpha_{f,pc}/(m_{nps} + m_{pc}) = \alpha_{f,pc}/m_{pc}(1 + K_f)$,. Similarly, we obtain $J_{f,nps} = \alpha_{f,nps}/m_{pc}(1 + K_f)$ using the 711 cm^{-1} band. Therefore, to obtain $J_{f,nps}$ and $J_{f,pc}$ values, we have to know the K_f value in advance.

The K_f value is obtained as follows. On the basis of the mass balance equation, $m_{nps} + m_{pc} + nm_{Zn} = m_T$ ($n = n_{nps} + n_{pc}$), we obtain the following relationship as:

$$I_{f,nps} = J_{f,nps} m_{nps} = J_{f,nps}(m_T - nm_{Zn}) - (J_{f,nps}/J_{f,pc}) I_{f,pc} \quad (2)$$

If the total solvation number of the metal ion and the intrinsic scattering coefficients are kept constant over a temperature range examined, the plot of $I_{f,nps}$ against $I_{f,pc}$ at varying temperature gives a straight line, and the slope gives the $J_{f,nps}/J_{f,pc}$. On the other hand, using the relationships $\ln K_f = \ln(I_{f,nps}/I_{f,pc}) - \ln(J_{f,nps}/J_{f,pc})$ and $-R \ln K_f = \Delta H°/T - \Delta S°$, we obtain

$$-R \ln(I_{f,nps}/I_{f,pc}) = \Delta H°/T - \Delta S° - R \ln(J_{f,nps}/J_{f,pc}) \quad (3)$$

The $\Delta H°$ and $-\Delta S° - R \ln(J_{f,nps}/J_{f,pc})$ values are evaluated from the slope and intercept, respectively, of the $-R \ln(I_{f,nps}/I_{f,pc})$ vs T^{-1} plots. The $\Delta S°$ value is evaluated by using the $J_{f,nps}/J_{f,pc}$ value separately obtained. The K_f value is calculated by using enthalpy and entropy values thus obtained.

Similarly, we define equilibrium constant $K_b = n_{nps}/n_{ps}$ and intrinsic scattering coefficients according to $I_{b,nps} = J_{b,nps} n_{nps} m_{Zn}$ and $I_{f,pc} = J_{b,pc} n_{pc} m_{Zn}$ for respective conformers bound to the metal ion, where $I_{b,nps}$ and $I_{b,pc}$ are band intensities at 727 and 776 cm^{-1}, respectively. The K_b, $\Delta H°$, and $\Delta S°$ values are obtained from the $-R \ln(I_{b,nps}/I_{b,pc})$ vs T^{-1} plots.

DFT Calculations. Here, for DFT calculations of DMPA and the Zn(II)−DMPA 1:2 cluster, we employed Becke's three-parameter hybrid method[36] with the Lee−Yang−Parr correlation[37,38] (B3LYP) and the 6-31G(d) basis set, and torsion energy profiles as a function of the C−C−C−O dihedral angle θ of DMPA were obtained. We also employed the B3LYP using basis sets with an effective core potential approximation, CEP-31G and CEP-121G(d,p),[39−41] which have an advantage to reduce not only computational time and cost, but also the basis set superposition error (BSSE). According to Zhou,[42] ab initio HF, MP2, and density functional theory BLYP and B3LYP methods with basis sets ranging from 6-31G* to 6-311+G(2d,p) give almost the same molecular structure and vibrational frequencies for DMF, although the result of MO calculations of *N*,*N*-dialkylamide strongly depends on the basis set.[43] Full geometry optimizations at the B3LYP/CEP-31G level followed by frequency analyses were then carried out for the $[Zn(\text{planar } cis\text{-DMPA})_{4-n}(\text{nonplanar staggered DMPA})_n]^{2+}$ ($n = 0-4$). The optimized geometries with no imaginary frequencies were

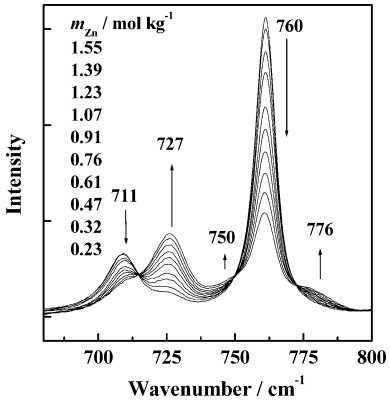

Figure 1. Raman spectra of DMPA containing varying molality of $Zn(ClO_4)_2$.

successfully obtained for all the solvates. All of the DFT calculations were carried out using Gaussian98[44] and Gaussian03[45] program suites.

Result and Discussions

Solvation Number of the Zinc(II) Ion in DMPA. A series of Raman spectra obtained by varying molality of $Zn(ClO_4)_2$ in DMPA are depicted in Figure 1. Each spectrum can be deconvoluted into five single bands with maxima at 711, 727, 750, 760, and 776 cm^{-1}, all of which are assigned to intramolecular vibrations of DMPA. The 711 and 760 cm^{-1} bands are ascribed to the N−CH_3 stretching vibration of free nonplanar staggered and planar cis conformers, respectively, in the bulk solvent. [31,46] The 727 and 776 cm^{-1} bands are assigned to the corresponding vibrations of the conformers bound to the metal ion. The vibration of each conformer in the bulk thus shifts to a higher frequency by 16 cm^{-1}, when it binds to the metal ion. The magnitude of shift is almost to the same extent as that found in the $Mn(ClO_4)_2$ and $Ca(ClO_4)_2$ DMPA solutions. The 750 cm^{-1} band, which was not found in previous works for the $Mn(ClO_4)_2$ and $Ca(ClO_4)_2$ DMPA solutions, probably owing to their relatively low salt molality, is ascribed to the nonplanar staggered conformer bound to the metal ion, as will be discussed later. The 760 cm^{-1} band is significantly stronger than that of the 711 cm^{-1} band, suggesting that the planar cis conformer is preferred to the nonplanar staggered one in the bulk solvent. On the other hand, intensity of the 727 cm^{-1} band is significantly stronger than that of the 776 cm^{-1} band, implying that the nonplanar staggered conformer is preferred in the coordination sphere of the zinc(II) ion, as well as the manganese(II) ion.[31]

Integrated intensities I_f of the free 711 and 760 cm^{-1} bands are plotted against the molality m_{Zn} of the zinc(II) ion in Figure 2. All experimental points fell on a straight line, and the solvation number of the zinc(II) ion was evaluated according to the procedure described in the Experimental Section. The solvation numbers thus obtained are 4.3 ± 0.3 and 3.9 ± 0.2 from the 711 and 760 cm^{-1} bands, respectively. If experimental uncertainty is taken into account, the solvation number of the zinc(II) ion in DMPA is 4, which is appreciably less than that of the manganese(II) ion. This is expected because the former ion is smaller than the latter.

According to our EXAFS[11] and Raman spectroscopy,[29] the solvation number of the zinc(II) ion is 6 in *N*,*N*-dimethylformamide (DMF), while it is 4.6, i.e., 6- and 4-solvated metal ions coexist in equilibrium, in *N*,*N*-dimethylacetamide (DMA). The zinc(II) ion is 4-solvated in hexamethylphosphoric triamide (HMPA)[26,27] and 1,1,3,3-tetramethylurea (TMU),[47] both of which involve the −$N(CH_3)_2$ group with similar bulkiness to the ethyl group. The solvation number thus decreases with increasing bulkiness of the functional group, particularly in the vicinity of the coordinating atom of solvent. Solvation steric effect, or steric hindrance among solvent molecules bound to the metal ion, thus seems to play a crucial role in the solvation number difference.

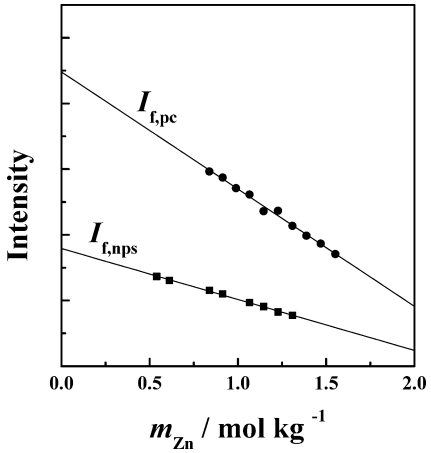

Figure 2. The I_f vs. m_{Zn} plots for the planar cis (●) and nonplanar staggered (■) conformers of DMPA.

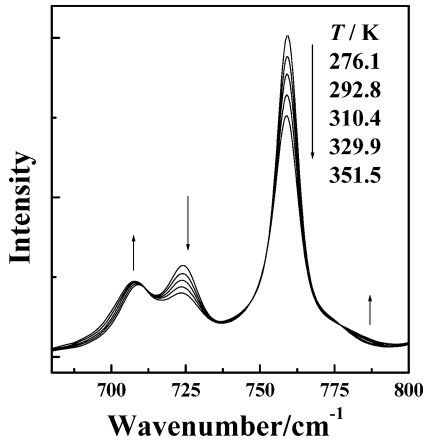

Figure 3. Variation of Raman spectra of DMPA containing 0.8 mol kg^{-1} $Zn(ClO_4)_2$ with raising temperature.

Conformational Equilibria of DMPA. Raman spectra of a $Zn(ClO_4)_2$ DMPA solution measured at varying temperature are shown in Figure 3. As seen, with rising temperature, the band intensity of the nonplanar staggered conformer in the bulk (711 cm^{-1}) increases, while that of the planar cis conformer (760 cm^{-1}) decreases. In contrast, the band intensity of the nonplanar staggered conformer bound to the metal ion (727 cm^{-1}) decreases, while that of the planar cis conformer (776 cm^{-1}) increases. This indicates that the nonplanar staggered conformer becomes more favorable in the bulk, but unfavorable in the coordination sphere, with increasing temperature. The equilibrium constant K ($=m_{nps}/m_{pc}$) and the enthalpy and entropy changes from planar cis to nonplanar staggered were then evaluated according to the procedure as described in the Experimental Section. Plots of $-R\ln(I_{f,pc}/I_{f,nps})$ and $-R\ln(I_{b,pc}/I_{b,nps})$ against T^{-1} are shown in Figure 4, and the slope gives the enthalpy change, which is positive for free DMPA and negative for bound DMPA. Plots of $I_{f,nps}$ against $I_{f,pc}$ at varying temperature, the slope of which gives the ratio $J_{f,nps}/J_{f,pc}$, also fall on a straight line. The Raman scattering coefficients at 298 K are listed in Table 1. The $J_{f,pc}$ and $J_{f,nps}$ values of 0.43 and 0.27, respectively, are in good agreement with those previously obtained.[31] The $J_{b,nps}$ value is significantly larger than the $J_{f,nps}$

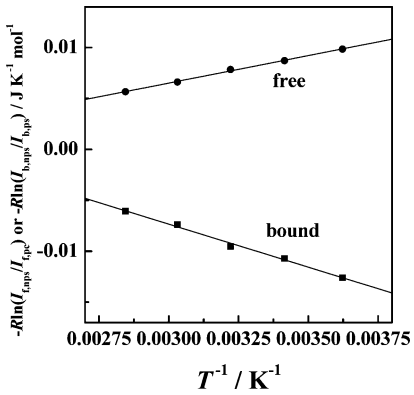

Figure 4. The $-R\ln(I_{f,nps}/I_{f,pc})$ and $-R\ln(I_{b,nps}/I_{b,pc})$ plots against T^{-1} for free (●) and bound (■) DMPA, respectively. The slope gives the $\Delta H°$ value of conformational change from planar cis to nonplanar staggered conformer.

TABLE 1: Solvation Number (n), Raman Scattering Coefficients (J_f and J_b) of Free and Bound *N,N*-Dimethylpropionamide, Respectively, and Raman Shift Relative to the Free Raman Band ($\Delta\nu$/cm^{-1} at 298 K)

Raman band/cm^{-1}	n	J_f	J_b	$\Delta\nu$
711.0 (nps)	4.3 ± 0.3[a]	0.27		
727.3 (nps)			0.39	16.3
760.0 (pc)	3.9 ± 0.2[a]	0.43		
776.0 (pc)			0.16	16.0

[a] Value refers to the standard deviation.

TABLE 2: The $\Delta G°$, $\Delta H°$, and $T\Delta S°$/kJ mol^{-1} of Conformational Change of DMPA from Planar Cis to Nonplanar Staggered Conformer in the Bulk Solvent and in the Coordination Sphere of the Metal Ion[a]

	$\Delta G°$	$\Delta H°$	$T\Delta S°$
bulk solvent	1.3(0.3)	5.4(0.2)	4.1(0.2)
Zn^{2+}	−0.9(0.6)	−8.5(0.4)	−7.5(0.4)
Mn^{2+} [b]	−1	−11	−10
Ca^{2+} [c]		−0.6	

[a] Values in parentheses refer to standard deviation. [b] Reference 7a. [c] Reference 7b.

value for the nonplanar staggered conformer, while the reverse is the case for the planar cis conformer. The $J_{b,nps}$ value for the nonplanar staggered conformer is significantly larger than the $J_{b,pc}$ for the planar cis one. The J_b values in the zinc(II) system differ appreciably from that in the manganese(II) system, implying that the value sensitively changes depending on the solvation number and the ionic radius of the metal ion.

The $\Delta G°$ ($=-RT\ln K$), $\Delta H°$, and $T\Delta S°$ values in the bulk solvent and in the coordination sphere of the zinc(II) ion are listed in Table 2, together with those in the coordination sphere of the manganese(II) and calcium ions. The $\Delta G°$, $\Delta H°$, and $T\Delta S°$ values obtained for the conformational change from planar cis to nonplanar staggered in the bulk are also in good agreement with those previously obtained.[31] The $\Delta H°$ value in the zinc(II) system is significantly negative unlike that in the bulk, indicating that the solvation steric effect does operate in the coordination sphere. The $\Delta H°$ values of −11 and 0.6 kJ mol^{-1} have been obtained for the manganese(II) and calcium ions, respectively.[31,32] As no specific ligand-field effect is expected for these metal ions, the $\Delta H°$ value does change strongly depending on the ionic radius and solvation number of the metal ion. To obtain more detailed insight into the solvation steric effect, we then carried out quantum mechanical calculations.

Torsion Energy Profile of the Propionyl Group. A partially optimized SCF energy for a single molecule of DMPA with a given C−C−C−O dihedral angle θ was calculated with use of B3LYP/CEP-31G and CEP-121G(d,p) basis sets, and the result is shown in Figure 5 as a function of θ, together with the result previously reported with use of the B3LYP/6-31G(d) basis set. As seen, there is no appreciable difference between energy profiles calculated by using the former two basis sets, although the values at $\theta = 60°$ and 90° are slightly lower than those calculated with use of the 6-31G(d) basis set. The global energy minimum appears at $\theta = 0°$ (the planar cis). The local minimum appears at $\theta = 90°$ (the nonplanar staggered), and the relative SCF energy is high by as much as ca. 5 kJ mol^{-1}. The SCF energy at $\theta = 180°$ (the planar trans) is even higher due to steric repulsion between terminal propionyl methyl and *N*-methyl groups, indicating that free rotation of the propionyl group is practically hindered.

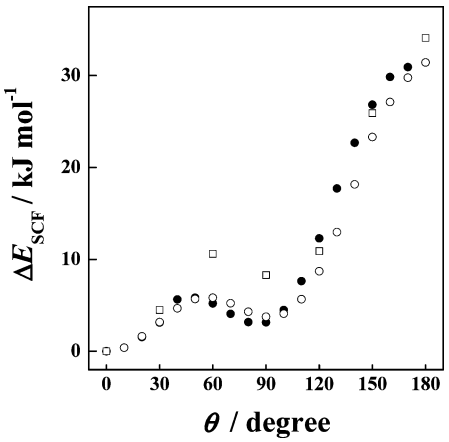

Figure 5. Torsion energy profiles as a function of the C−C−C−O dihedral angle θ for a single DMPA molecule calculated with 6-31G(d) (□), CEP-31G (●) and CEP-121G(d,p) (○) basis sets.

With use of the same basis sets, DFT calculations were then carried out for the Zn^{2+}−DMPA 1:2 cluster. Geometry optimizations followed by normal-mode analyses were carried out for both $[Zn(\text{planar cis DMPA})_2]^{2+}$ and $[Zn(\text{nonplanar staggered DMPA})_2]^{2+}$, and fully optimized geometries with no imaginary frequencies were obtained. It revealed that the energy of the $[Zn(\text{planar cis DMPA})_2]^{2+}$ corrected for the zero-point energy (ZPE) is −19.3 kJ mol^{-1} smaller than that of the $[Zn(\text{nonplanar staggered DMPA})_2]^{2+}$. Therefore, torsion energy profiles were calculated by fixing one solvent molecule to either the planar cis form (the propionyl C−C−C−O dihedral angle $\theta = 0.0°$) or the nonplanar staggered form ($\theta = 87.8°$ obtained for the $[Zn(\text{nonplanar staggered DMPA})_2]^{2+}$). The relative SCF energy profiles are shown in Figure 6. As seen, the energy profile is similar to that of the single DMPA molecule, as well as the protonated DMPA.[31] This implies that the conformational equilibrium of bound DMPA is hardly changed by electronic solvent−solvent interaction through the zinc(II) ion. However, the nonplanar staggered conformer is indeed preferred to the planar cis one in the coordination sphere of the zinc(II) ion in DMPA. This clearly indicates that steric solvent−solvent interaction through space or solvation steric effect plays a key role in the conformational equilibrium around the metal ion. Therefore, we further examined DFT calculations for the $Zn(DMPA)_4^{2+}$ solvate ion using the B3LYP/CEP-31G basis set.

DFT Calculations of $Zn(DMPA)_4^{2+}$. Geometry optimizations followed by frequency analyses were carried out for the $[Zn(\text{planar cis DMPA})_{4-n}(\text{nonplanar staggered DMPA})_n]^{2+}$ ($n = 0-4$) solvate ions. Local energy minima were also successfully obtained for these solvate ions without significant change in the conformation at the initial stage. All of the

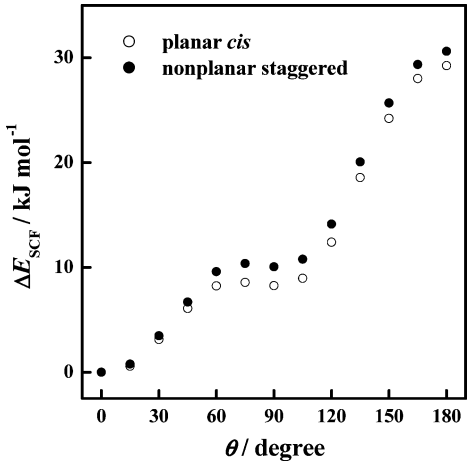

Figure 6. Torsion energy profiles as a function of the C−C−C−O dihedral angle θ for DMPA in the Zn(II)−DMPA 1:2 clusters with one DMPA molecule fixed at $\theta = 0°$ (○) and $\theta = 90°$ (●) calculated with the B3LYP/CEP-31G basis set.

TABLE 3: Structural Parameters for [Zn(planar cis DMPA)$_{4-n}$(nonplanar staggered DMPA)$_n$]$^{2+}$ Predicted by DFT Calculations, Using the B3LYP/CEP-31G Basis Set[a]

	N				
	0	1	2	3	4
Zn−O/100 pm	(1.9534)	(1.9596)	(1.9526)	(1.9574)	(1.9543)
	1.9544	1.9605	(1.9605)	(1.9630)	(1.9554)
	1.9541	1.9574	1.9687	(1.9543)	(1.9555)
	1.9549	1.9482	1.9501	1.9586	(1.9551)
average	1.9542	1.9564	1.9580	1.9583	1.9551
Zn−O−C	153.79	(140.59)	(139.78)	(138.09)	(141.40)
	153.12	150.95	(139.40)	(138.95)	(141.71)
	153.21	152.36	150.89	(138.61)	(141.28)
	153.75	152.56	150.79	150.65	(141.64)
average	153.47	149.12	145.22	141.58	141.51
Zn−O−C−N	175.74	(174.91)	(−179.32)	(−178.63)	(−175.59)
	−174.20	−169.58	(173.55)	(171.50)	(−173.86)
	175.60	−180.00	−175.05	(−179.92)	(171.69)
	−176.05	175.03	−177.91	179.13	(171.95)
average[b]	4.60	5.12	3.54	2.71	6.73

[a] Values in parentheses refer to the nonplanar staggered conformer. [b] Deviation from the planarity.

optimized structures show no imaginary frequencies, and the BSSE for the optimized structures was found to be negligible. Structural parameters, such as the Zn−O bond length, Zn−O−C bond angle, and Zn−O−C−N dihedral angle, are listed in Table 3. As seen, there is no significant difference in both bond length and dihedral angle among these solvates. With the Zn−O−C bond angle, on the other hand, the values are ca. 150° and 140° for the planar cis and nonplanar staggered conformers, respectively, in the four-solvate complex. The respective angles in the Zn(II)−DMPA 1:2 cluster are 134° and 143°. The angle of the nonplanar staggered conformer is thus kept almost unchanged, while that of the planar cis one increases significantly in the four-solvate complex. This implies that the planar cis conformer is more sterically hindered in the four-solvate complex.

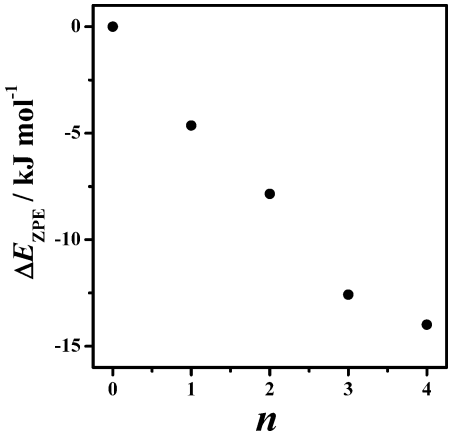

Figure 7. Relative ZPE corrected energies for [Zn(planar cis DMPA)$_{4-n}$(nonplanar staggered DMPA)$_n$]$^{2+}$ obtained by DFT calculations with the B3LYP/CEP-31G basis set.

CHART 2: Optimized Geometry of [Zn(planar cis DMPA)$_2$(nonplanar staggered DMPA)$_2$]$^{2+}$

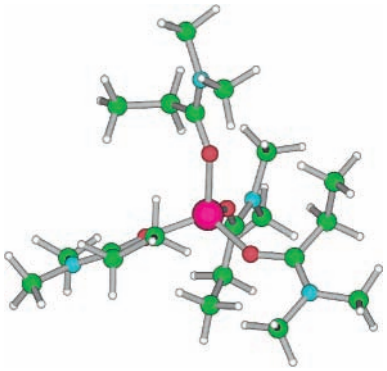

The ZPE corrected energy of [Zn(planar cis DMPA)$_{4-n}$(nonplanar staggered DMPA)$_n$]$^{2+}$ ($n = 0-4$) relative to that of [Zn(planar cis DMPA)$_4$]$^{2+}$, ΔE_{ZPE}, is plotted in Figure 7. Typical geometry of the [Zn(planar cis DMPA)$_2$(nonplanar staggered DMPA)$_2$]$^{2+}$ complex is shown in Chart 2. The energy of the four-solvate complex monotonically decreases with *n*, indicating that the steric repulsion becomes weaker by replacing the planar cis conformer with the nonplanar staggered one. The slope (ca. −3.6 kJ mol^{-1}) may give an enthalpy of planar cis to nonplanar

TABLE 4: Frequencies (ν/cm^{-1}) and Raman Scattering Activity (ψ/(Å^4/amu)) of Predicted Raman Bands of [Zn(planar cis DMPA)$_{4-n}$(nonplanar staggered DMPA)$_n$]$^{2+}$ ($n = 0-4$) in the Region 680−800 cm^{-1} Obtained by DFT Calculations, Using the B3LYP/CEP-31G Basis Set[a]

$n = 0$		$n = 1$		$n = 2$		$n = 3$		$n = 4$	
ν	ψ	ν	ψ	ν	ψ	ν	ψ	ν	ψ
759.76	7.42	(706.93)	(1.88)	(706.00)	(5.42)	(705.28)	(3.28)	(704.07)	(1.18)
760.34	0.38	(732.39)	(5.99)	(709.28)	(9.96)	(707.03)	(4.30)	(705.86)	(0.99)
760.60	7.68	758.86	4.29	(728.01)	(4.38)	(709.82)	(16.73)	(706.58)	(9.10)
765.50	44.41	760.71	6.12	(733.89)	(4.62)	(729.22)	(3.82)	(709.23)	(22.14)
		763.77	0.37	758.01	8.59	(735.31)	(3.56)	(726.53)	(4.96)
				761.81	23.37	736.49	6.66	(728.75)	(4.63)
						759.49	17.05	(734.64)	(0.31)
								(735.00)	(9.69)

[a] Values in parentheses refer to the nonplanar staggered conformer.

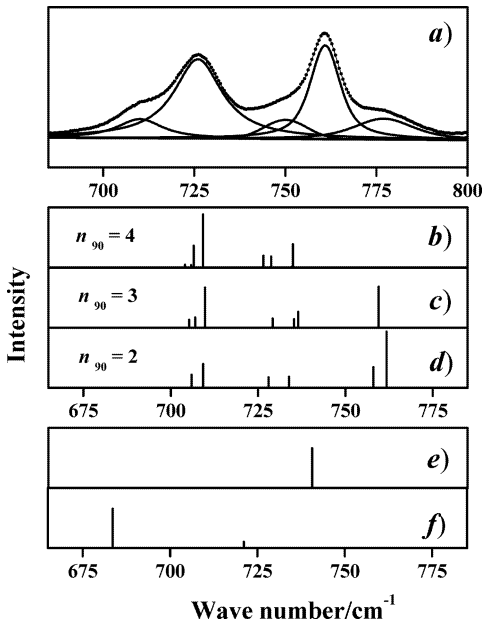

Figure 8. The observed Raman spectrum of DMPA containing 1.58 mol kg^{-1} $Zn(ClO_4)_2$ (a) and predicted Raman bands obtained by DFT calculation, using the B3LYP/CEP-31G basis set: [Zn(planar cis DMPA)$_{4-n}$(nonplanar staggered DMPA)$_n$]$^{2+}$ with $n = 4$ (b), 3 (c), and 2(d), and single planar cis (e) and nonplanar staggered (f) conformers.

staggered conformational change. The value is in fairly good agreement with the experimental one (−8.5 kJ mol^{-1}), if we take into account the precision of the DFT calculations.

On the basis of optimized geometries of [Zn(planar cis DMPA)$_{4-n}$(nonplanar staggered DMPA)$_n$]$^{2+}$, their vibrational frequencies were calculated. The values thus obtained in the region of 680−800 cm^{-1} are listed in Table 4 and also shown in Figure 8. The single planar cis conformer is predicted to show a Raman band at 740 cm^{-1}, while the nonplanar staggered conformer shows bands at 683 and 721 cm^{-1}, although predicted bands are systematically shifted to lower frequencies by ca. 20−30 cm^{-1}. The bound planar cis and nonplanar staggered conformers are predicted to show Raman bands at 761 and 707 cm^{-1}, respectively. The magnitudes of frequency shift upon binding to the metal ion are 20 and 14 cm^{-1} for the planar cis and nonplanar staggered conformers, respectively, which are in good agreement with the observed ones. On the other hand, the calculated scattering activity cannot reproduce the observed intensity, implying that intermolecular solvent−solvent interactions in the second coordination sphere may also play a significant role in the band intensity.

We thus propose that there exists the [Zn(planar cis DMPA)$_{4-n}$ (nonplanar staggered DMPA)$_n$]$^{2+}$ ion in DMPA, and the nonplanar staggered conformer is more favorable in the coordination sphere. The relative ΔE_{ZPE} energy difference among solvates of $n = 2-4$ is not large, and these solvate ions may coexist in equilibrium at room temperature. We thus conclude that a steric interaction among DMPA molecules still operates even in the four-coordinate solvate ion.

Acknowledgment. This work has been financially supported by Grant-in-Aids for Scientific Research 13440222 and 15750052 from the Ministry of Education, Culture, Sports, Science and Technology of Japan, and also by a Grant for Basic Science Research Project from the Sumitomo Foundation. DFT calculations have partly been carried out with a GS320 computer at the Computing and Communications Center, Kyushu University.

References and Notes

(1) Marcus, Y. *Ion Solvation*; Wiley: New York, 1985. Marcus, Y. *Ion Properties*; Marcel Decker: New Yor, 1997.
(2) Ohtaki, H.; Radnai, T. *Chem. Rev.* **1993**, *93*, 1157.
(3) Ohtaki, H.; Radnai, T.; Yamaguchi, T. *Chem. Soc. Rev.* **1997**, *26*, 41.
(4) Ohtaki, H. *Monatsh. Chem.* **2001**, *132*, 1237.
(5) Funahashi, S.; Inada, Y. *Trends Inorg. Chem.* **1998**, *5*, 15.
(6) Funahashi, S.; Inada, Y. *Bull. Chem. Soc. Jpn.* **2002**, *75*, 1901.
(7) Ishiguro, S. *Pure Appl. Chem.* **1994**, *66*, 393−398.
(8) Ishiguro, S. *Bull. Chem. Soc. Jpn.* **1997**, *70*, 1465.
(9) Ishiguro, S.; Umebayashi, Y.; Komiya, M. *Coord. Chem. Rev.* **2002**, *226*, 103−111.
(10) Ishiguro, S.; Umebayashi, Y.; Kanzaki, R. *Anal. Sci.*, **2004**, *20*, 415−421.
(11) Ozutsumi, K.; Koide, M.; Suzuki, H.; Ishiguro, S. *J. Phys. Chem.* **1993**, *97*, 500−502.
(12) Koide, M.; Suzuki, H.; Ishiguro, S. *J. Solution Chem.* **1994**, *23*, 1257.
(13) Koide, M.; Ishiguro, S. *Z. Naturforsch. A* **1995**, *50*, 11.
(14) Koide, M.; Ishiguro, S. *J. Solution Chem.* **1995**, *24*, 511.
(15) Koide, M.; Ishiguro, S. *J. Chem. Soc., Faraday Trans.* **1995**, *91*, 2313.
(16) Koide, M.; Suzuki, H.; Ishiguro, S. *J. Chem. Soc., Faraday Trans.* **1995**, *91*, 3851.
(17) Koide, M.; Suzuki, H.; Ishiguro, S. *J. Solution Chem.* **1996**, *25*, 1261.
(18) Suzuki, H.; Ishiguro, S. *Acta Crystallogr. C* **1997**, *C53*, 1602.
(19) Ishiguro, S.; Umebayashi, Y.; Komiya, M. *Coord. Chem. Rev.* **2002**, *226*, 103.
(20) Umebayashi, Y.; Komiya, M.; Nagahama, Y.; Kobayashi, H.; Ishiguro, S. *J. Chem. Soc., Faraday Trans.* **1998**, *94*, 647.
(21) Ishiguro, S.; Umebayashi, Y.; Kato, K.; Takahashi, R.; Ozutsumi, K. *J. Chem. Soc., Faraday Trans.* **1998**, *94*, 3607.
(22) Ishiguro, S.; Umebayashi, Y.; Kato, K.; Nakasone, S.; Takahashi, R. *Phys. Chem. Chem. Phys.* **1999**, *1*, 2725.
(23) Abe, Y.; Ozutsumi, K.; Ishiguro, S. *J. Chem. Soc., Faraday Trans. 1* **1989**, *85*, 3747.
(24) Abe, Y.; Ishiguro, S. *J. Solution Chem.* **1991**, *20*, 793.
(25) Abe, Y.; Takahashi, R.; Ishiguro, S.; Ozutsumi, K. *J. Chem. Soc., Faraday Trans.* **1992**, *88*, 1997.
(26) Ozutsumi, K.; Tohji, K.; Udagawa, Y.; Abe, Y.; Ishiguro, S. *Inorg. Chim. Acta* **1992**, *191*, 183.
(27) Ozutsumi, K.; Abe, Y.; Takahashi, R.; Ishiguro, S. *J. Phys. Chem.* **1994**, *98*, 9894.
(28) Umebayashi, Y.; Matsumoto, K.; Watanabe, M.; Katoh, K.; Ishiguro, S. *Anal. Sci.* **2001**, *17*, 323.
(29) Umebayashi, Y.; Matsumoto, K.; Watanabe, M.; Ishiguro, S. *Phys. Chem. Chem. Phys.* **2001**, *3*, 5475.
(30) Umebayashi, Y.; Matsumoto, K.; Mekata, I.; Ishiguro, S. *Phys. Chem. Chem. Phys.* **2002**, *4*, 5599.
(31) Umebayashi, Y.; Matsumoto, K.; Mune, Y.; Zhang, Y.; Ishiguro, S. *Phys. Chem. Chem. Phys.* **2003**, *5*, 2552.
(32) Umebayashi, Y.; Mune, Y.; Tsukamoto, T.; Zhang, Y.; Ishiguro, S. *J. Mol. Liq.* **2005**, *118*, 45.
(33) Marquardt, D. W. *J. Soc. Ind. Appl. Math.* **1963**, *11*, 431.
(34) Press: W. H.; Flannery, B. P.; Teukolsky, S. A.; Vetterling, W. T. *Numerical Recipes*; Cambridge University Press: Cambridge, UK, 1989.
(35) McCreery, R. L. *Raman Spectroscopy for Chemical Analysis*; Wiley-Interscience: New York, 2000.
(36) Becke, A. D. *J. Chem. Phys.* **1993**, *98*, 5648.
(37) Lee, C.; Yang, W.; Parr, R. G. *Phys. Rev. B* **1988**, *37*, 785.
(38) Miehlich, B.; Savin, A.; Stoll, H.; Preuss, H. *Chem. Phys. Lett.* **1989**, *157*, 200.
(39) Stevens, W.; Basch, H.; Krauss, J. *J. Chem. Phys.* **1984**, *81*, 6026.
(40) Stevens, W. J.; Krauss, M.; Basch, H.; Jasien, P. G. *Can. J. Chem.* **1982**, *70*, 612.
(41) Cundari, T. R.; Stevens, W. J. *J. Chem. Phys.* **1993**, *98*, 5555.
(42) Zhou, X.; Krauser, J. A.; Tate, D. R.; VanBuren, Al. S.; Clark, J. A.; Moody, P. R.; Liu, R. *J. Phys. Chem.*, **1996**, *100*, 16822−16827.
(43) Foresman, J. B.; Frisch, Æ. *Exploring Chemistry With Electronic Structure Methods*, 2nd ed.; Gaussian, Inc.: Pittsburgh, PA, 1996.
(44) Frisch, M. J.; Trucks, G. W.; Schlegel, H. B.; Scuseria, G. E.; Robb, M. A.; Cheeseman, J. R.; Zakrzewski, V. G.; Montgomery, J. A., r.; Stratmann, R. E.; Burant, J. C.; Dapprich, S.; Millam, J. M.; Daniels, A. D.; Kudin, K. N.; Strain, M. C.; Farkas, O.; Tomasi, J.; Barone, V.; Cossi, M.; Cammi, R.; Mennucci, B.; Pomelli, C.; Adamo, C.; Clifford, S.; Ochterski, J.; Petersson, G. A.; Ayala, P. Y.; Cui, Q.; Morokuma, K.; Malick, D. K.; Rabuck, A. D.; Raghavachari, K.; Foresman, J. B.; Cioslowski, J.; Ortiz, J. V.; Baboul, A. G.; Stefanov, B. B.; Liu, G.; Liashenko, A.; Piskorz, P.; Komaromi, I.; Gomperts, R.; Martin, R. L.; Fox, D. J.; Keith, T.; Al-

Laham, M. A.; Peng, C. Y.; Nanayakkara, A.; Challacombe, M.; Gill, P. M. W.; Johnson, B.; Chen, W.; Wong, M. W.; Andres, J. L.; Gonzalez, C.; Head-Gordon, M.; Replogle, E. S.; Pople, J. A. *Gaussian 98*, Rev. A.9, Gaussian, Inc.: Pittsburgh, PA, 1998.

(45) Frisch, M. J.; Trucks, G. W.; Schlegel, H. B.; Scuseria, G. E.; Robb, M. A.; Cheeseman, J. R.; Montgomery, J. A., Jr.; Vreven, T.; Kudin, K. N.; Burant, J. C.; Millam, J. M.; Iyengar, S. S.; Tomasi, J.; Barone, V.; Mennucci, B.; Cossi, M.; Scalmani, G.; Rega, N.; Petersson, G. A.; Nakatsuji, H.; Hada, M.; Ehara, M.; Toyota, K.; Fukuda, R.; Hasegawa, J.; Ishida, M.; Nakajima, T.; Honda, Y.; Kitao, O.; Nakai, H.; Klene, M.; Li, X.; Knox, J. E.; Hratchian, H. P.; Cross, J. B.; Adamo, C.; Jaramillo, J.; Gomperts, R.; Stratmann, R. E.; Yazyev, O.; Austin, A. J.; Cammi, R.; Pomelli, C.; Ochterski, J. W.; Ayala, P. Y.; Morokuma, K.; Voth, G. A.; Salvador, P.; Dannenberg, J. J.; Zakrzewski, V. G.; Dapprich, S.; Daniels, A. D.; Strain, M. C.; Farkas, O.; Malick, D. K.; Rabuck, A. D.; Raghavachari, K.; Foresman, J. B.; Ortiz, J. V.; Cui, Q.; Baboul, A. G.; Clifford, S.; Cioslowski, J.; Stefanov, B. B.; Liu, G.; Liashenko, A.; Piskorz, P.; Komaromi, I.; Martin, R. L.; Fox, D. J.; Keith, T.; Al-Laham, M. A.; Peng, C. Y.; Nanayakkara, A.; Challacombe, M.; Gill, P. M. W.; Johnson, B.; Chen, W.; Wong, M. W.; Gonzalez, C.; Pople, J. A. *Gaussian 03*, Rev. B.04; Gaussian, Inc.: Pittsburgh, PA, 2003.

(46) Murugan, R.; Mohan, S. *Spectrochim. Acta, A* **1995**, *51*, 735.

(47) Inada, Y.; Sugimoto, K.; Ozutsumi, K.; Funahashi, S. *Inorg. Chem.* **1994**, *33*, 1875−1880.